

IMPLEMENTATION OF MUR'S ABSORBING BOUNDARIES WITH PERIODIC STRUCTURES TO SPEED UP THE DESIGN PROCESS USING FINITE-DIFFERENCE TIME-DOMAIN METHOD

G. Zheng, A. A. Kishk, A. W. Glisson, and A. B. Yakovlev

Department of Electrical Engineering
Center for Applied Electromagnetic Systems Research (CAESR)
University of Mississippi
University, MS 38677, USA

Abstract—The finite-difference time-domain (FDTD) method is used to obtain numerical solutions of infinite periodic structures without resorting to the complex frequency-domain analysis, which is required in traditional frequency-domain techniques. The field transformation method is successfully used to model periodic structures with oblique incident waves/scan angles. Maxwell's equations are transformed so that only a single period of the infinite periodic structure is modeled in FDTD by using periodic boundary conditions (PBCs). When modeling periodic structures with the transformed fields, the standard Mur second-order absorbing boundary condition cannot be used directly to absorb the outgoing waves. This paper presents a new implementation of Mur's second-order absorbing boundary condition (ABC) with the transformed fields in the FDTD method. For designs that require multi-parametric studies, Mur's ABCs are efficient and sufficient boundary conditions. If more accurate results are needed, the perfectly matched layer (PML) ABC can be used with the parameters obtained from the Mur solution.

1. INTRODUCTION

The finite-difference time-domain (FDTD) method has been widely used for the analysis of electromagnetic scattering, radiation, and propagation problems since it was first introduced by Yee [1]. The FDTD method is simple and accurate without resorting to the somewhat more complex traditional frequency-domain techniques, such as Method of Moments (MoM). It has the capability to

simulate electromagnetic interactions in complicated geometries that are extremely difficult to analyze by other methods. Due to the limitations of computational resources, the FDTD numerical solution requires the use of radiation or absorbing boundary conditions (ABCs) in order to accurately truncate an infinite computational domain. One of the analytical ABC methods developed for open-boundary problems is based on the one-way wave equations (OWWEs). Engquist and Majda proposed the use of OWWEs for truncation of the computational domain [2] and Mur introduced the discretization and application of OWWEs to the Yee algorithm [3]. Before the Perfectly Matched Layer (PML) ABCs were developed in [4], Mur's second-order ABC and its modifications were among the most widely used ABCs in the FDTD method.

In many electromagnetic applications, the structures of interest have a periodicity in one or two dimensions, such as frequency selective surfaces (FSS) [5], electromagnetic bandgap (EBG) structures [6], or infinite antenna arrays [7]. To apply the FDTD method to the oblique incidence case for such structures, the field transformation method was introduced in [8]. Its further extensions can be found in [9, 10]. One of the FDTD discretization methods for the transformed fields is the split-field method [11–13]. The field transformation method is applied to transform Maxwell's equations from the E - H domain to the mapped P - Q domain. In addition, this method can be used in FDTD to overcome difficulties in the implementation of time-advance and time-delay across the grid [14]. In this case, infinite periodic structures are truncated into single-period structures with periodic boundary conditions (PBCs) in one or two dimensions. The other sides of the computational domain in FDTD must be truncated by ABCs to avoid reflections. Due to structural periodicities, the ABCs should have periodic properties so that they can properly absorb the outgoing waves. In contrast, the standard Mur second-order ABC needs proper adjustments in order to absorb the outgoing waves.

This paper proposes a new discretization method of Mur's second-order ABC with transformed fields in FDTD. A key feature of the method is to separate the FDTD updating equations in Mur's second-order ABC into two parts. Each part is updated by different components. In the normal incidence case, however, the proposed Mur second-order ABC in the mapped P - Q domain retains its standard form as in the E - H domain.

2. FORMULATIONS AND EQUATIONS

Consider a periodic structure that may contain lossy, anisotropic materials with periodicities in both the y - and z -directions, and which is truncated by ABCs in the x -direction. In the frequency domain, the field transformation method is applied to transform the electric and magnetic field components from the E - H domain to the P - Q domain as,

$$\tilde{P}_x = \tilde{E}_x e^{jk_y y + jk_z z}, \quad (1a)$$

$$\tilde{P}_y = \tilde{E}_y e^{jk_y y + jk_z z}, \quad (1b)$$

$$\tilde{P}_z = \tilde{E}_z e^{jk_y y + jk_z z}, \quad (1c)$$

$$\tilde{Q}_x = \eta_0 \tilde{H}_x e^{jk_y y + jk_z z}, \quad (1d)$$

$$\tilde{Q}_y = \eta_0 \tilde{H}_y e^{jk_y y + jk_z z}, \quad (1e)$$

$$\tilde{Q}_z = \eta_0 \tilde{H}_z e^{jk_y y + jk_z z}. \quad (1f)$$

The tilde symbol “ \sim ” is used to denote the field components in the frequency domain. After substituting these transformed field components into Maxwell’s equations and transforming them from the frequency domain to the time domain, the modified time-dependent Maxwell’s equations can be obtained [9, 10] (the derivation are given in the Appendix for convenience,

$$\frac{\partial}{\partial t} \left(\frac{\epsilon_r}{c} \vec{P} + \frac{1}{c} \Lambda \times \vec{Q} \right) = \nabla \times \vec{Q} - \vec{R} \quad (2a)$$

$$\frac{\partial}{\partial t} \left(\frac{\mu_r}{c} \vec{Q} - \frac{1}{c} \Lambda \times \vec{P} \right) = -\nabla \times \vec{P} - \vec{R}_m \quad (2b)$$

where

$$\begin{aligned} \vec{P} &= P_x \hat{x} + P_y \hat{y} + P_z \hat{z} \\ \vec{Q} &= Q_x \hat{x} + Q_y \hat{y} + Q_z \hat{z} \\ \Lambda &= k_y \hat{y} + k_z \hat{z} \\ k_y &= \sin \theta \sin \phi \\ k_z &= \cos \theta \\ \vec{R} &= \sigma \eta_0 \vec{P} \\ \vec{R}_m &= \frac{\sigma^*}{\eta_0} \vec{Q} \end{aligned}$$

and θ , ϕ represent the incident/scan angles in the problem.

Using the modified Maxwell's equations (2) and following the procedure presented in [2], the free-space one-way wave equation in the mapped P - Q domain can be obtained as [8, 10],

$$\left(\frac{\partial^2}{\partial x^2} + \frac{\partial^2}{\partial y^2} - 2k_y \frac{\partial^2}{\partial y \partial t} + k_y^2 \frac{\partial^2}{\partial t^2} + \frac{\partial^2}{\partial z^2} - 2k_z \frac{\partial^2}{\partial z \partial t} + k_z^2 \frac{\partial^2}{\partial t^2} - \frac{\partial^2}{c^2 \partial t^2} \right) W = 0 \quad (3)$$

where W represents field quantity that is tangential to the absorbing boundary in the P - Q domain.

The computational domain in FDTD is truncated at $x = 0$ and $x = h$ in the x -direction with ABCs, and the ABCs with transformed fields at these two planes become

$$\begin{aligned} \frac{\partial^2 W}{\partial x \partial t} - \frac{1}{c} \left(1 - \frac{k_y^2}{2} - \frac{k_z^2}{2} \right) \frac{\partial^2 W}{\partial t^2} + \frac{c}{2} \left(\frac{\partial^2 W}{\partial y^2} + \frac{\partial^2 W}{\partial z^2} \right) \\ - \frac{1}{\partial t} \left(k_y \frac{\partial W}{\partial y} + k_z \frac{\partial W}{\partial z} \right) = 0, \text{ at } x = 0 \end{aligned} \quad (4a)$$

and

$$\begin{aligned} \frac{\partial^2 W}{\partial x \partial t} + \frac{1}{c} \left(1 + \frac{k_y^2}{2} + \frac{k_z^2}{2} \right) \frac{\partial^2 W}{\partial t^2} - \frac{c}{2} \left(\frac{\partial^2 W}{\partial y^2} + \frac{\partial^2 W}{\partial z^2} \right) \\ + \frac{1}{\partial t} \left(k_y \frac{\partial W}{\partial y} + k_z \frac{\partial W}{\partial z} \right) = 0, \text{ at } x = h. \end{aligned} \quad (4b)$$

In the following, the absorbing boundary at $x = 0$ is discretized in FDTD as an example. The other boundary is also developed in a similar way.

2.1. Mur's First-order ABCs

Because the first-order Mur ABC in FDTD removes both the y - and z -derivative terms, the periodic properties of the structures in OWWEs will also be removed. Therefore, the discretized form of the first-order Mur ABC in FDTD at $x = 0$ will be the same as the standard one [14],

$$W|_{0,j,k}^{n+1} = W|_{1,j,k}^n + \frac{c\Delta t - \Delta x}{c\Delta t + \Delta x} \left(W|_{1,j,k}^{n+1} - W|_{0,j,k}^n \right) \quad (5a)$$

or

$$\begin{aligned} W|_{0,j}^{n+1} = -W|_{1,j}^{n-1} + \frac{c\Delta t - \Delta x}{c\Delta t + \Delta x} \left(W|_{1,j}^{n+1} - W|_{0,j}^{n-1} \right) \\ + \frac{2\Delta x}{c\Delta t + \Delta x} \left(W|_{0,j}^n + W|_{1,j}^n \right) \end{aligned} \quad (5b)$$

where i, j, k represent the grid positions in the x -, y - and z -directions in the computational domain, and n represents the iteration time step.

2.2. Mur's Second-order ABCs

Following standard procedures in the discretization of Mur's second-order ABC in FDTD creates difficulties in discretizing some terms in equation (3) that combine both the y - and z -derivative and the time-derivative, that are introduced by the field transformation method. Therefore, it is convenient to rewrite equation (3) as

$$\frac{\partial^2 W}{\partial x \partial t} - \frac{1}{c} \left(1 - \frac{k_y^2}{2} - \frac{k_z^2}{2} \right) \frac{\partial^2 W}{\partial t^2} + \frac{c}{2} \left(\frac{\partial^2 W}{\partial y^2} + \frac{\partial^2 W}{\partial z^2} \right) - \frac{1}{\partial t} \left(k_y \frac{\partial W}{\partial y} + k_z \frac{\partial W}{\partial z} \right) = 0. \quad (6a)$$

Equation (6a) is separated into two parts,

$$f(W) = \frac{\partial^2 W}{\partial x \partial t} - \frac{1}{c} \left(1 - \frac{k_y^2}{2} - \frac{k_z^2}{2} \right) \frac{\partial^2 W}{\partial t^2} + \frac{c}{2} \left(\frac{\partial^2 W}{\partial y^2} + \frac{\partial^2 W}{\partial z^2} \right) \quad (6b)$$

$$g(W) = \frac{1}{\partial t} \left(k_y \frac{\partial W}{\partial y} + k_z \frac{\partial W}{\partial z} \right). \quad (6c)$$

In this case, $f(W)$ can be discretized by using the standard Mur procedure to obtain

$$\begin{aligned} & \left(\frac{1}{\Delta t \Delta x} + \frac{1}{c \Delta t^2} \left(1 - \frac{k_y^2}{2} - \frac{k_z^2}{2} \right) \right) W|_{0,j,k}^{n+1} \\ &= \frac{1}{\Delta t} \left(\frac{W|_{1,j,k}^{n+1}}{\Delta x} - \frac{W|_{1,j,k}^{n-1} - W|_{0,j,k}^{n-1}}{\Delta x} \right) \\ & - \frac{1}{c} \left(1 - \frac{k_y^2}{2} - \frac{k_z^2}{2} \right) \left(\frac{-2W|_{0,j,k}^n + W|_{0,j,k}^{n-1}}{\Delta t^2} \right. \\ & \quad \left. + \frac{W|_{1,j,k}^{n+1} - 2W|_{1,j,k}^n + W|_{1,j,k}^{n-1}}{\Delta t^2} \right) \\ & + \frac{c}{2} \left(\left(\frac{W|_{0,j+1,k}^n - 2W|_{0,j,k}^n + W|_{0,j-1,k}^n}{\Delta y^2} \right) \right. \\ & \quad \left. + \frac{W|_{1,j+1,k}^n - 2W|_{1,j,k}^n + W|_{1,j-1,k}^n}{\Delta y^2} \right) \end{aligned}$$

$$+ \left(\begin{array}{c} \frac{W|_{0,j,k+1}^n - 2W|_{0,j,k}^n + W|_{0,j,k-1}^n}{\Delta z^2} \\ + \frac{W|_{1,j,k+1}^n - 2W|_{1,j,k}^n + W|_{1,j,k-1}^n}{\Delta z^2} \end{array} \right) \quad (7a)$$

In the field transformation method, we choose the dual-time technique [9, 11] to update fields in FDTD. Thus, we can update $g(W)$ as

$$g(W) = \frac{k_y}{2} \left(\begin{array}{c} \frac{(W|_{1,j+1,k}^{n+1/2} - W|_{1,j-1,k}^{n+1/2}) - (W|_{1,j+1,k}^{n-1/2} - W|_{1,j-1,k}^{n-1/2})}{2\Delta y\Delta t} \\ + \frac{(W|_{0,j+1,k}^{n+1/2} - W|_{0,j-1,k}^{n+1/2}) - (W|_{0,j+1,k}^{n-1/2} - W|_{0,j-1,k}^{n-1/2})}{2\Delta y\Delta t} \end{array} \right) \\ + \frac{k_z}{2} \left(\begin{array}{c} \frac{(W|_{1,j,k+1}^{n+1/2} - W|_{1,j,k-1}^{n+1/2}) - (W|_{1,j,k+1}^{n-1/2} - W|_{1,j,k-1}^{n-1/2})}{2\Delta z\Delta t} \\ + \frac{(W|_{0,j,k+1}^{n+1/2} - W|_{0,j,k-1}^{n+1/2}) - (W|_{0,j,k+1}^{n-1/2} - W|_{0,j,k-1}^{n-1/2})}{2\Delta z\Delta t} \end{array} \right). \quad (7b)$$

By combining the two parts together, we obtain the final updating equation for Mur's second-order ABC,

$$\left(\frac{1}{\Delta t\Delta x} + \frac{1}{c\Delta t^2} \left(1 - \frac{k_y^2}{2} - \frac{k_z^2}{2} \right) \right) W|_{0,j,k}^{n+1} = \\ \frac{1}{\Delta t} \left(\frac{W|_{1,j,k}^{n+1}}{\Delta x} - \frac{W|_{1,j,k}^{n-1} - W|_{0,j,k}^{n-1}}{\Delta x} \right) \\ - \frac{1}{c} \left(1 - \frac{k_y^2}{2} - \frac{k_z^2}{2} \right) \left(\begin{array}{c} \frac{-2W|_{0,j,k}^n + W|_{0,j,k}^{n-1}}{\Delta t^2} \\ + \frac{W|_{1,j,k}^{n+1} - 2W|_{1,j,k}^n + W|_{1,j,k}^{n-1}}{\Delta t^2} \end{array} \right) \\ + \frac{c}{2} \left(\begin{array}{c} \left(\frac{W|_{0,j+1,k}^n - 2W|_{0,j,k}^n + W|_{0,j-1,k}^n}{\Delta y^2} \right. \\ \left. + \frac{W|_{1,j+1,k}^n - 2W|_{1,j,k}^n + W|_{1,j-1,k}^n}{\Delta y^2} \right) \\ + \left(\frac{W|_{0,j,k+1}^n - 2W|_{0,j,k}^n + W|_{0,j,k-1}^n}{\Delta z^2} \right. \\ \left. + \frac{W|_{1,j,k+1}^n - 2W|_{1,j,k}^n + W|_{1,j,k-1}^n}{\Delta z^2} \right) \end{array} \right)$$

$$\begin{aligned}
& -k_y \left(\frac{\left(W|_{1,j+1,k}^{n+1/2} - W|_{1,j-1,k}^{n+1/2} \right) - \left(W|_{1,j+1,k}^{n-1/2} - W|_{1,j-1,k}^{n-1/2} \right)}{2\Delta y \Delta t} \right. \\
& \quad \left. + \frac{\left(W|_{0,j+1,k}^{n+1/2} - W|_{0,j-1,k}^{n+1/2} \right) - \left(W|_{0,j+1,k}^{n-1/2} - W|_{0,j-1,k}^{n-1/2} \right)}{2\Delta y \Delta t} \right) \\
& -k_z \left(\frac{\left(W|_{1,j,k+1}^{n+1/2} - W|_{1,j,k-1}^{n+1/2} \right) - \left(W|_{1,j,k+1}^{n-1/2} - W|_{1,j,k-1}^{n-1/2} \right)}{2\Delta z \Delta t} \right. \\
& \quad \left. + \frac{\left(W|_{0,j,k+1}^{n+1/2} - W|_{0,j,k-1}^{n+1/2} \right) - \left(W|_{0,j,k+1}^{n-1/2} - W|_{0,j,k-1}^{n-1/2} \right)}{2\Delta z \Delta t} \right).
\end{aligned} \tag{7c}$$

3. NUMERICAL VERIFICATIONS

In this section, numerical validations based on the formulations described in Section 2 are presented. In the first numerical experiment, we consider a y - and z -periodic infinite infinitesimal-dipole array with scan angle (normal scan angle). The grid sizes in the x -, y -, and z -directions are 0.5 mm, and the time step is 0.77 ps. The computational domain in the x -, y -, and z -directions is 15 cm \times 25 cm \times 25 cm (30 \times 50 \times 50 cells). The dimensions in the periodic directions are larger than in the absorbing direction so that the coupling fields from neighboring unit cells arrive to the sampling positions later than fields reflected from the ABCs. A larger benchmark domain (100 \times 50 \times 50 cells) truncated by a 10-layer PML is used as the reference for the reflection studies of Mur's ABCs. A horizontal infinitesimal dipole is placed in the center of the computational domain, (15, 25, 25), with a Gaussian waveform pulse peaking at time-step $n = 73$ with a peak value of 1 as

$$P_y(t) = \exp\left(-\frac{(t-t_0)^2}{\tau^2}\right) \tag{8}$$

where t_0 is the time at which the pulse reaches its maximum and τ is a parameter related to pulse width. To study the reflections from ABCs, global error [14] is not used here due to the limitation of computer resources and complexity of the field transformation method. Instead, a local normalized error at the observation point (1, 15, 15) and an averaged normalized error at the observation plane $x = 1$ are defined in (9) and (10)

$$Local_Error(t) = \frac{|y(t) - y_{reference}(t)|}{\max |y_{reference}(t)|} \tag{9}$$

$$Avg_Error(t) = Avg \left(\frac{|y(t) - y_{reference}(t)|}{\max |y_{reference}(t)|} \right) \Big|_{x=1}. \quad (10)$$

Since $c\Delta t \approx \Delta x/2$, the leading edge of the propagating wave generated by the source requires approximately $116\Delta t$ to propagate from the source to the observation point $(1, 15, 15)$ and approximately $103\Delta t$ to propagate over the $15\Delta t$ distance to the center of the plane grid at $x = 1$, or $(1, 25, 25)$. The strong coupling fields from the nearest neighboring unit cells will arrive at approximately $167\Delta t$. This allows the outgoing wave to pass through the boundaries and excite the possible reflections from the boundaries.

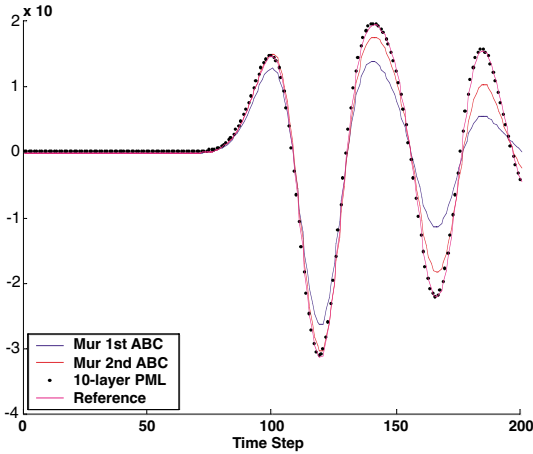
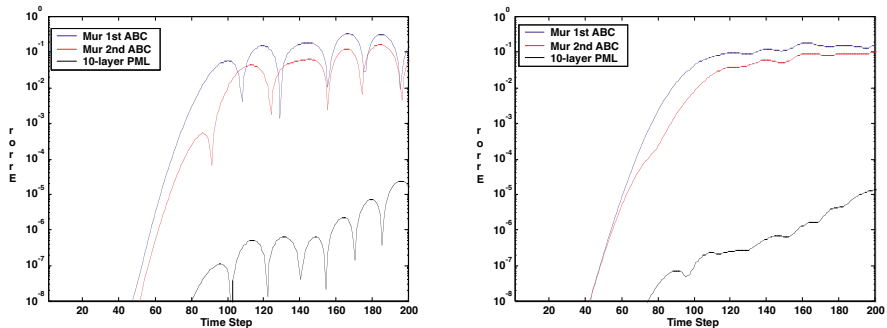


Figure 1. Time-domain response from Mur’s first-order, second-order ABCs and PML ABCs over the first 200 time steps for normal scan angle.

Fig. 1 shows the time-domain responses from Mur’s first-order, second-order ABCs and 10-layer PML ABCs for the case of normal scan angle. In Fig. 1, the time-domain result obtained by using the Mur second-order ABC is much closer to the reference result than that of the Mur first-order ABC, as expected. Fig. 2 compares both the local error and averaged error among the Mur first-order, second-order ABCs and 10-layer PML ABCs over 200 time steps. The Mur second-order ABC yields approximately 1/3 of local error and approximately 1/2 of averaged error of the Mur first-order ABC. After the coupling fields from the neighboring unit cells become significant, the differences between Mur’s first-order and second-order ABCs are smaller. The computational time and memory requirement for Mur’s first-order, second-order ABCs and 10-layer PML ABCs are listed as Table 1.

Table 1. Computational resources required for Mur's 1st order, Mur's 2nd order ABCs and 10-layer PML ABCs.

	Mur's 1 st order ABCs	Mur's 2 nd order ABCs	10-layer PML ABCs
Memory (Mb)	24	25	38
CPU time (s)	37	38	58

**Figure 2.** Reflection errors from Mur's first-order, second-order ABCs and PML ABCs over the first 200 time steps for normal scan angle: (a) local errors, (b) averaged errors.

A second numerical validation is conducted at 45° scan angle with the same computational domain, excitation form, and sampling positions as in the previous case. The requirements for stability condition and the dispersion relation in FDTD at this angle are the most restrictive among all the scan angles [13]. The time step is changed to 0.42ps for this case in order to satisfy the stability condition, which depends on the scan angle. The leading edge of the propagating wave generated by the source requires approximately $210\Delta t$ to propagate from the source to the observation point $(1, 15, 15)$ and approximately $187\Delta t$ to propagate over the $15\Delta t$ distance to the center of the plane grid at $x = 1$, or $(1, 25, 25)$. The strong coupling fields from the nearest neighboring unit cells will arrive at approximately $304\Delta t$.

Fig. 3 shows the time-domain response of Mur's first-order, second-order ABCs and 10-layer PML ABCs for the case of the 45 -degree scan angle. The time-domain result obtained by using the Mur second-order ABC is much closer to the reference result than the result of the Mur first-order ABC, which is similar to the previous case. This

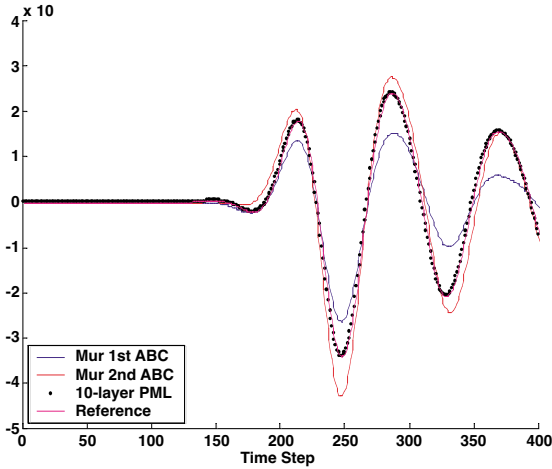


Figure 3. Time-domain response from Mur's first-order, second-order ABCs and PML ABCs over the first 400 time steps for the 45-degree scan angle.

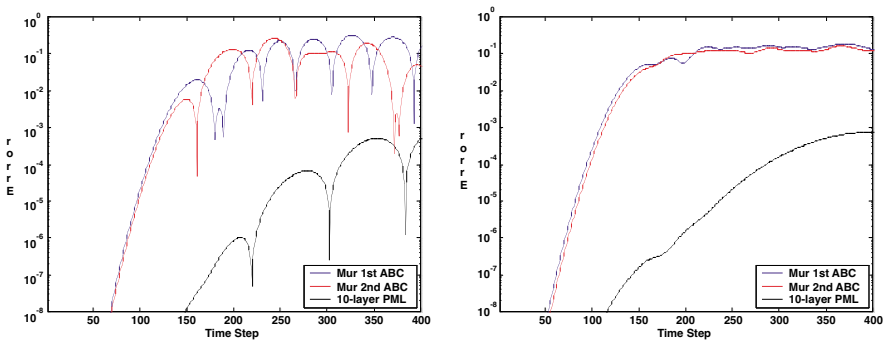


Figure 4. Reflection errors from Mur's first-order, second-order ABCs and PML ABCs over the first 400 time steps for the 45-degree scan angle: (a) local errors, (b) averaged errors.

indicates that Mur's second-order ABCs generate less reflection than the first-order ABCs for the oblique scan angle. Fig. 4 compares both the local error and averaged error among the Mur first-order, second-order ABCs and 10-layer PML ABCs over 400 time steps. Mur's second-order ABC yields approximately 2/5 of the local error and approximately 2/3 of averaged error of Mur's first-order ABC. The local and averaged errors at 45-degree scan angle are larger than those

obtained in the case of the normal scan angle. At 45-degree scan angle, the numerical value of wave velocity is not equal to the value of free-space wave velocity, which is used in both Mur's first-order and second-order ABCs. From the updating equations, the effect on Mur's second-order ABCs is larger than that of the first-order. The reflection errors from Mur's second-order ABC can be reduced if the actual numerical value of the wave velocity is used in the updating equations. Another reason is that some weaker coupling fields have already arrived at the sampling positions before $304\Delta t$ have affected the reflection studies.

4. CONCLUSION

Mur's first-order and second-order ABCs with periodic boundary conditions have been implemented in the FDTD method in order to analyze periodic structures. Based on the numerical experiments, Mur's first-order and second-order ABCs require 50% less memory, 50algorithm than a 10-layer PML ABCs with the same computational domain. Mur's second-order ABC is more accurate than the first-order ABC and can be successfully applied for a multi-parametric quick design with periodicities.

ACKNOWLEDGMENT

This work was partially supported by The Army Research Office under grant No. DAAD19-02-1-0074.

APPENDIX A. MODIFIED MAXWELL'S EQUATIONS IN THE P - Q DOMAIN

Define the transformed fields as

$$\tilde{P}_x = \tilde{E}_x e^{jk_y y + jk_z z}, \quad (\text{A1a})$$

$$\tilde{P}_y = \tilde{E}_y e^{jk_y y + jk_z z}, \quad (\text{A1b})$$

$$\tilde{P}_z = \tilde{E}_z e^{jk_y y + jk_z z}, \quad (\text{A1c})$$

$$\tilde{Q}_x = \eta_0 \tilde{H}_x e^{jk_y y + jk_z z}, \quad (\text{A1d})$$

$$\tilde{Q}_y = \eta_0 \tilde{H}_y e^{jk_y y + jk_z z}, \quad (\text{A1e})$$

$$\tilde{Q}_z = \eta_0 \tilde{H}_z e^{jk_y y + jk_z z}, \quad (\text{A1f})$$

which are used in the frequency domain Maxwell's equations to yield

$$\frac{j\omega\varepsilon_{xr}}{c}\vec{P}_x + \sigma_x\eta_0\vec{P}_x = \frac{\partial\vec{Q}_z}{\partial y} - \frac{\partial\vec{Q}_y}{\partial z} - j\vec{k}_y\frac{\partial}{\partial t}\vec{Q}_z + j\vec{k}_z\vec{Q}_y \quad (\text{A2a})$$

$$\frac{j\omega\varepsilon_{yr}}{c}\vec{P}_y + \sigma_y\eta_0\vec{P}_y = -\frac{\partial\vec{Q}_z}{\partial x} + \frac{\partial\vec{Q}_x}{\partial z} - j\vec{k}_z\vec{Q}_x \quad (\text{A2b})$$

$$\frac{j\omega\varepsilon_{zr}}{c}\vec{P}_z + \sigma_z\eta_0\vec{P}_z = \frac{\partial\vec{Q}_y}{\partial x} - \frac{\partial\vec{Q}_x}{\partial y} + j\vec{k}_y\vec{Q}_x \quad (\text{A2c})$$

$$\frac{j\omega\mu_{xr}}{c}\vec{Q}_x + \frac{\sigma_x^*}{\eta_0}\vec{Q}_x = -\frac{\partial\vec{P}_z}{\partial y} + \frac{\partial\vec{P}_y}{\partial z} + j\vec{k}_y\vec{P}_z - j\vec{k}_z\vec{P}_y \quad (\text{A2d})$$

$$\frac{j\omega\mu_{yr}}{c}\vec{Q}_y + \frac{\sigma_y^*}{\eta_0}\vec{Q}_y = \frac{\partial\vec{P}_z}{\partial x} - \frac{\partial\vec{P}_x}{\partial z} + j\vec{k}_z\vec{P}_x \quad (\text{A2e})$$

$$\frac{j\omega\mu_{zr}}{c}\vec{Q}_z + \frac{\sigma_z^*}{\eta_0}\vec{Q}_z = -\frac{\partial\vec{P}_y}{\partial x} + \frac{\partial\vec{P}_x}{\partial y} - \vec{k}_y\vec{P}_x \quad (\text{A2f})$$

Transformation of equation (A2) from frequency domain into time domain yields

$$\frac{\varepsilon_{xr}}{c}\frac{\partial P_x}{\partial t} + \sigma_x\eta_0 P_x = \frac{\partial Q_z}{\partial y} - \frac{\partial Q_y}{\partial z} - \frac{k_y}{c}\frac{\partial Q_z}{\partial t} + \frac{k_z}{c}\frac{\partial Q_y}{\partial t} \quad (\text{A3a})$$

$$\frac{\varepsilon_{yr}}{c}\frac{\partial P_y}{\partial t} + \sigma_y\eta_0 P_y = -\frac{\partial Q_z}{\partial x} + \frac{\partial Q_x}{\partial z} - \frac{k_z}{c}\frac{\partial Q_x}{\partial t} \quad (\text{A3b})$$

$$\frac{\varepsilon_{zr}}{c}\frac{\partial P_z}{\partial t} + \sigma_z\eta_0 P_z = \frac{\partial Q_y}{\partial x} - \frac{\partial Q_x}{\partial y} + \frac{k_y}{c}\frac{\partial Q_x}{\partial t} \quad (\text{A3c})$$

$$\frac{\mu_{xr}}{c}\frac{\partial Q_x}{\partial t} + \frac{\sigma_x^*}{\eta_0}Q_x = -\frac{\partial P_z}{\partial y} + \frac{\partial P_y}{\partial z} + \frac{k_y}{c}\frac{\partial P_z}{\partial t} - \frac{k_z}{c}\frac{\partial P_y}{\partial t} \quad (\text{A3d})$$

$$\frac{\mu_{yr}}{c}\frac{\partial Q_y}{\partial t} + \frac{\sigma_y^*}{\eta_0}Q_y = \frac{\partial P_z}{\partial x} - \frac{\partial P_x}{\partial z} + \frac{k_z}{c}\frac{\partial P_x}{\partial t} \quad (\text{A3e})$$

$$\frac{\mu_{zr}}{c}\frac{\partial Q_z}{\partial t} + \frac{\sigma_z^*}{\eta_0}Q_z = -\frac{\partial P_y}{\partial x} + \frac{\partial P_x}{\partial y} - \frac{k_y}{c}\frac{\partial P_x}{\partial t} \quad (\text{A3f})$$

where $\hat{k} = \sin\theta\cos\phi\hat{x} + \sin\theta\sin\phi\hat{y} + \cos\theta\hat{z} = k_x\hat{x} + k_y\hat{y} + k_z\hat{z}$.

By rewriting equation (A3), a compact form of the modified Maxwell's equations in time domain can be obtained as

$$\frac{\partial}{\partial t}\left(\frac{\varepsilon_r}{c}\vec{P} + \frac{1}{c}\Lambda \times \vec{Q}\right) = \nabla \times \vec{Q} - \vec{R} \quad (\text{A4a})$$

$$\frac{\partial}{\partial t}\left(\frac{\mu_r}{c}\vec{Q} - \frac{1}{c}\Lambda \times \vec{P}\right) = -\nabla \times \vec{P} - \vec{R}_m \quad (\text{A4b})$$

REFERENCES

1. Yee, K. S., "Numerical solution of initial boundary value problems involving Maxwell's equations in isotropic media," *IEEE Trans. Antenn. Propagat.*, Vol. AP-14, No. 3, 302–307, 1966.
2. Engquist, B. and A. Majda, "Absorbing boundary conditions for the numerical simulation of waves," *Math. Comp.*, Vol. 31, No. 139, 629–651, 1977.
3. Mur, G., "Absorbing boundary conditions for the finite-difference approximation of the time-domain electromagnetic-field equations," *IEEE Trans. Electromagn. Compat.*, Vol. EMC-23, No. 4, 377–382, 1981.
4. Berenger, J. P., "A perfectly matched layer for the absorption of electromagnetic waves," *J. Comput. Phys.*, Vol. 114, 185–200, 1994.
5. Munk, B. A., *Frequency Selective Surfaces: Theory and Design*, John Wiley, New York 2000.
6. Yablonovitch, E., "Photonic band-gap structures," *J. Opt. Soc. Amer. B.*, Vol. 10, No. 2, 283–294, 1993.
7. Maloney, J. G. and M. P. Kesler, "Analysis of antenna arrays using the split-field update FDTD method," *Proc. IEEE AP-S Int. Symp.*, Vol. 4, 2036–2039, 1998.
8. Veysoglu, M. E., R. T. Shin, and J. A. Kong, "A finite-difference time-domain analysis of wave scattering from periodic surfaces: oblique incident case," *J. Electromagnetic Waves and Applications*, Vol. 7, No. 12, 1595–1607, 1993.
9. Kao, Y. C. A. and R. G. Atkins, "A finite difference-time domain approach for frequency selective surfaces at oblique incidence," *Proc. IEEE AP-S Int. Symp.*, Vol. 2, 1432–1435, 1996.
10. Kao, Y. C. A., "Finite-difference time domain modeling of oblique incidence scattering from periodic surfaces," Thesis, Massachusetts Institute of Technology, 1997.
11. Roden, J. A., "Electromagnetic analysis of complex structures using the FDTD technique in general curvilinear coordinates," Ph.D. Thesis, University of Kentucky, Lexington, KY, 1997.
12. Roden, J. A., S. D. Gedney, M. P. Kesler, J. G. Maloney, and P. H. Harms "Time-domain analysis of periodic structures at oblique incidence: Orthogonal and nonorthogonal FDTD implementations," *IEEE trans. Microwave Theory and Techniques*, Vol. 46, 420–427, 1998.
13. Harms, P. H., J. A. Roden, J. G. Maloney, M. P. Kesler, E. J. Kuster, and S. D. Gedney, "Numerical analysis of periodic

- structures using the split-field algorithm,” *Proc. 13th Annual Review of Progress in Applied Computational Electromagnetics*, 104–111, 1997.
14. Taflov, A. and S. C. Hagness, *Computational Electromagnetics: the Finite-Difference Time-Domain Method*, 2nd ed., Artech House, Norwood, 2000.